

Development of a rule to maximize the research octane number (RON) of the isomerization product from light naphtha

Reza Hayati^{*,†}, Sorood Zahedi Abghari^{*}, Sepehr Sadighi^{**}, and Mahmood Bayat^{***}

^{*}Process Development and Control Group, Research Institute of Petroleum Industry (RIPI), P. O. Box 14665137, Tehran, Iran

^{**}Catalysis and Nanotechnology Research Division, Research Institute of Petroleum Industry (RIPI),
P. O. Box 14665137, Tehran, Iran

^{***}Faculty of Research and Development in Downstream Petroleum Industry, Research Institute of Petroleum Industry (RIPI),
P. O. Box 14665137, Tehran, Iran

(Received 1 February 2014 • accepted 22 August 2014)

Abstract—The isomerization process is a substantial technology to produce clean fuel from linear paraffinic species existing in light naphtha. We investigated the influence of hydrocracking reactions besides the other reactions on the research octane number (RON) of the isomerization product. A reaction network and a kinetic model including fifteen lumps and sixteen reactions were developed. Several experiments were carried out in a pilot plant to estimate kinetic parameters. The accuracy of the model was evaluated by comparing the model prediction with the experimental results. The maximum RON and process yield were strongly dependent on the temperature, hydrogen to hydrocarbon molar ratio (H₂/Oil) and liquid hourly space velocity (LHSV). Also, increasing the reaction temperature compensated for the negative effects of raising the LHSV and H₂/Oil in RON maximization. Moreover, we concluded that the hydro cracking reactions were very effective on RON, such that they can dominate the role of the other reactions. By sensitivity analysis in this research, a rule was obtained to declare the effect of operating condition on maximization of RON and the method of revamping of naphtha isomerization reactor.

Keywords: Isomerization, Optimal Operation, Kinetic Model, RON, Light Naphtha

INTRODUCTION

Crude oil refining complexes have faced stringent environmental regulations that limit the concentration of aromatic compounds in gasoline (Euro-4 and Euro-5). Hence, the naphtha isomerization process has gained attention for its ability to substitute aromatic components with other species. This process is useful to decrease the aromatic components in the gasoline pool by converting them to iso-paraffinic species [1].

In a typical light-naphtha isomerization process, hydrogen and light naphtha, mainly including straight chain (normal) paraffinic hydrocarbons (nP), are fed from the top of a fixed-bed catalytic reactor, and move downward throughout the bed. During the isomerization, most of the normal paraffinic hydrocarbons with low octane number are converted to the iso-paraffins with the same carbon, but higher octane number. However, the same as the other catalytic processes, deactivation of catalyst by coke formation or poisoning is the main challenge [2].

Active catalysts of the isomerization process have high acidic characteristic, which allows the formation of highly reactive intermediates, and leads to forming the desired isomerized species [3,4]. The catalyst normally used in this process has zeolite or is chlorinated alumina based [5-10]. They are in bead or extrudate form and usu-

ally contain between 0.2 and 0.4 wt% of platinum [6]. For processing of heavy naphtha containing C₇ and C₈, the (metal)/SO₄²⁻/ZrO₂ catalyst is useful for carrying out the isomerization reactions at lower operating temperature and higher yield [7]. In this issue, several works were carried out to improve the catalyst structure and increase the yield of the isomerization process using the modified catalyst formulation [8-10].

Similar to other refining and petrochemical processes [11-13], optimal operation is required to guarantee profitability and productivity, and it necessitates using process models. Therefore, a kinetic model can be beneficial to finding the optimum operating conditions. This model is also used to investigate the effect of operating variables, i.e., temperature, recycle flow rate, pressure, hydrogen-to-hydrocarbon ratio and fluid velocity on the process yield and product quality [14]. Moreover, a model can be applied to upscale or precise control and automation [15]. With respect to these concepts, many studies have been carried out to develop kinetic-based models for isomerization processes [16-21].

In previous-works, linear paraffinic isomerization, ring opening and benzene saturation reactions were only included in the model. So, the effect of operating variables such as temperature, hydrogen to hydrocarbon molar ratio and reactor residence time was investigated using the mentioned reactions [22,23]. Consequently, the optimum temperature was obtained by the consideration of thermodynamic and kinetic constraints of linear paraffinic isomerization reactions without including the effect of hydrocracking reactions [24,25].

[†]To whom correspondence should be addressed.

E-mail: Hayatir@Ripi.ir, reza.hayati@gmail.com

Copyright by The Korean Institute of Chemical Engineers.

The main contribution of the present research was to study the effect of hydrocracking reactions on the light naphtha isomerization process. To do such a task, several experiments were carried out in a pilot scale plant using different type of feedstock over a wide range of operating conditions. Based on these results, a reaction network consisting of linear paraffin isomerization, naphtha ring opening, benzene saturation and hydrocracking reaction was developed. After proposing a rigorous kinetic model, we explored the impact of the momentous process variables, such as temperature, type of feed stock, hydrogen-to oil molar ratio and LHSV (liquid hourly space velocity), on the yield and octane number of the product.

EXPERIMENTAL DEVICES AND MATERIALS

1. Pilot Plant

The experiments were conducted in the pilot catalyst system (Geomecanique BL-2) which was licensed by Institut Francais du Petrole. This device is in the Research Institute of the Petroleum Industry (RIPI), and it can tolerate temperatures and pressures up to 500 °C and 300 bar, respectively. A picture and a simplified diagram of the experimental devices are presented in Figs. 1 and 2, respectively. For each experiment, the reactor was loaded with 20 ml of catalyst with the diameter of 2 to 3 mm, diluted with the equal percentage of inert quartz particles. To have a better distribution through the bed, the top and bottom of the catalytic bed were charged with 2.5 mm of quartz particles with the diameter of 2-4 mm.

To analyze the product gas stream, an Agilent gas chromatograph (GC) device (model 6890) was used. The liquid product was analyzed using DHA (detailed hydrocarbon analysis) according to ASTM D-5134 standard procedure.

2. Catalyst

In the present research, a commercial Pt/Zeolite type catalyst for light naphtha isomerization was used. The characteristics of the fresh catalyst are presented in Table 1. Before loading, the catalyst was heated to 130 °C and then held at this temperature for about 6 h for drying. After drying and catalyst loading, nitrogen was introduced to replace the air in the reactor system. Then, hydrogen was introduced to the reactor to replace the nitrogen up to pressurize



Fig. 1. The set up for the isomerization tests located in research institute of petroleum industry (RIPI).

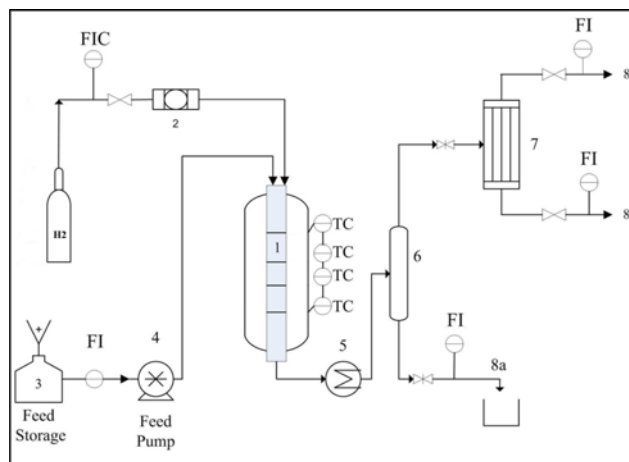


Fig. 2. Simplified flow diagram from the pilot plant from which the experimental data were taken.

FIC. Flow indicator controller	FI. Flow indicator
TI. Temperature indicator	TC. Temperature controller
1. Reactor	6. Gas-liquid separator
2. Gas dryer	7. Light gas condenser
3. Light naphtha feed storage	8a, 8b and 8c. Liquid and gas products
4. Feed pump	
5. Condenser	

Table 1. Characteristics and specifications of the isomerization catalyst studied

Ingredients of catalyst	Si, Pt, Ca, Fe, Ti
Pt content (wt%)	0.28-0.3
Properties of catalyst	
Shape	Extrudate
Diameter (mm)	2-3
Surface area (m ² /g)	450
Pore volume (cm ³ /g)	0.4
Average pore radius (°A)	40
Bulk density (kg/m ³)	~0.7
Loss of ignition@520 °C (wt%)	<5
Abrasion loss (%)	0.2-0.3
Crushing strength (kPa/mm)	>130

the system to operating pressure which can reach to 80 bar. Then, the catalyst bed was heated with the temperature ramp of 10 °C/min, and kept at 420 °C for 2 h.

3. Feed Stock Specifications

The isomerization feed stock was taken from a commercial isomerization unit. The feed properties are shown in Table 2.

4. Operating Conditions

The variables with the greatest impact on the operation of the isomerization process, i.e., reactor temperature, hydrogen to hydrocarbon molar ratio and LHSV, are presented in Table 3. Since the operating pressure in the process is almost constant (except at the end of catalyst life time in which the coke is formed), the pressure in the pilot experiments is kept constant and equal to 25 bar, which is equal to industrial operating conditions. Based on the range of

Table 2. Analysis of the different feedstock

Component	FeedStock1 (mol%)	FeedStock2 (mol%)	FeedStock3 (mol%)	FeedStock4 (mol%)	FeedStock5 (mol%)	FeedStock6 (mol%)
IP5	8.654	5.177	5.246	1.650	4.343	1.981
NP5	30.780	26.953	27.370	16.746	30.669	16.740
5N5	0.747	0.826	0.526	0.950	0.539	0.718
22DMB	0.211	0.172	0.109	1.143	0.318	0.295
23DMB	1.751	1.111	2.436	3.980	3.137	3.560
2MC5	9.703	8.070	14.872	20.453	15.320	17.668
3MC5	7.457	9.356	14.687	17.221	12.251	13.969
NP6	20.372	28.640	23.550	23.656	22.060	25.579
5N6	13.536	15.206	8.743	10.414	8.835	13.706
6N6	4.217	3.291	1.679	3.054	1.824	4.311
A6	0.827	0.000	0.748	0.497	0.687	0.998
1-Butene	0.000	0.127	0.000	0.000	0.000	0.000
NP7	0.116	0.033	0.002	0.015	0.001	0.023
2MC6	0.447	0.081	0.005	0.047	0.002	0.055
3MC6	0.406	0.085	0.005	0.042	0.002	0.055

Table 3. The range of operating condition of light naphtha isomerization experiments

Operating condition	
Reactor inlet temperature (°C)	200-260
LHSV (hr ⁻¹)	0.9-2
Hydrogen over feed molar ratio	1.2-2

the operating variables, the isomerization process was performed under the conditions reported in Table 5.

MODEL DEVELOPMENT

Fifteen lumps and sixteen reactions were considered in the pro-

posed network, which is presented in Fig. 3. Among these reactions, isomerization and hydrogenation were irreversible. Corresponding to this network, a kinetic model was developed, and all reactions rates were assumed as power law equation. Thereafter, the related kinetic parameters were estimated using the obtained experimental data from the pilot scale plant.

The one-dimensional plug flow reactor hypothesis was assumed to model the fixed bed isomerization reactor. Furthermore, it was supposed that the reactor works under isothermal and non-adiabatic conditions. The mass conservation equations for each component can be written as follows:

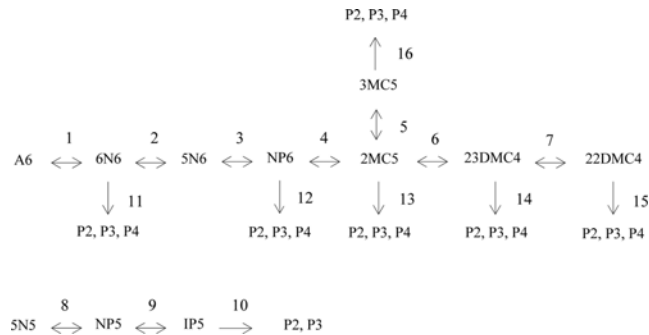
$$\frac{dF_i}{dz} = \sum_{k=1}^l R_{ik} \quad (1)$$

Table 4. The rate constants of the isomerization reaction network

Reactions	k _f	k _r	E _f (kJ/kgmole)	E _r (kJ/kgmole)	
1	A6+3H ₂ ↔6N6	0.011	0.0010	148.72	215.2
2	6N6↔5N6	0.0120	0.0013	167.36	180.4
3	5N6+H ₂ ↔NP6	0.0010	0.0001	278.93	356.4
4	NP6↔2MC5	0.0167	0.0014	114.07	790.4
5	2MC5↔3MC5	0.0130	0.0015	176.67	194.3
6	2MC5↔23DMC4	0.0110	0.0012	157.34	168.4
7	23DMC4↔22DMC4	0.0387	0.0269	14.743	961.9
8	5N5+H ₂ ↔NP5	0.0015	1.2×10 ⁻⁴	325.41	670.2
9	NP5↔IP5	0.0053	0.0012	107.29	714.9
10	IP5+H ₂ →P2+P3	0.0011	----	371.97	----
11	6N6+H ₂ →P2+P3+P4	1.4172×10 ⁻⁵	----	2746.2	----
12	NP6+H ₂ →P2+P3+P4	1.5026×10 ⁻⁶	----	3546.9	----
13	2MC5+H ₂ →P2+P3+P4	6.0334×10 ⁻⁵	----	1552.6	----
14	23DMC4+H ₂ →P2+P3+P4	0.0013	----	232.4	----
15	22DMC4+H ₂ →P2+P3+P4	0.0019	----	241.7	----
16	3MC5+H ₂ →P2+P3+P4	0.0147	----	440.4	----

Table 5. Case studies used for model evaluation

Case study	Feedstock	LHSV (h ⁻¹)	H2 to feed molar Ratio	Reactor Feedstock temperature (°C)
1	Feed 1	1.00	1.60	225
2	Feed 2	1.00	1.60	226
3	Feed 3	1.02	1.20	226
4	Feed 4	1.25	1.20	225
5	Feed 5	1.00	1.25	226
6	Feed 6	1.15	1.45	230

**Fig. 3. Isomerization reaction network.**

where F_i is the molar flux of i th species; R_{ik} is the reaction rate of i th species, and z is the height of catalyst in packed bed. As an example Eq. (1) for 2MC5 (2-methyl cyclo pentane) is as follows:

$$\frac{dF_{2MC5}}{dz} = R_{4-2MC5} - R_{5-2MC5} - R_{6-2MC5} \quad (2)$$

where the indexes of the rates demonstrated on the right hand side of the equation, refers to the number of the reactions illustrated in Table 4 and the 2MC5 as the species, which the mass equation is written about. Based on the isothermal assumption, the energy balance equation can be ignored. Consequently, the mass balance equations should be solved to model the isomerization reactor.

To determine the kinetic parameters of the proposed model, i.e., activation energy and frequency factors of sixteen reactions, the sum of the squared errors between the mole fraction of species at the outlet of the reactor and the predicted values by the model was minimized as follows:

$$\min \sum_{i=1}^N \omega_i \left| \frac{X_i^{Cal} - X_i^{Exp}}{X_i^{Exp}} \right| \quad (3)$$

w.r.t

$$k_{f,m}, k_{r,m}, E_{f,m}, E_{r,n} \quad (n=1, 2, \dots, 16)$$

Subject to:

$$\text{s.t. } h_j(x) = 0 \quad (j=1, 2, \dots, m) \quad (4)$$

where ω_i is the weighting factor; N is the number of species, and X_i^{cal} and X_i^{Exp} are the calculated and experimental mole fractions, respectively. Furthermore, constraints (3) express the equality for the optimization problem. It is obvious that the fitting parameters are the activation energy and frequency factors. To find the optimized values of these parameters, the Nelder-Mead algorithm of

the Matlab software (Mathworks, 2012a) was used.

To complete the modeling procedure, estimating of RON is essentially needed due to the role of this parameter for evaluating the performance of the isomerization process. This parameter is also an index for evaluating the catalyst activity. To do such a task, the Riazi method [26] is applied to predict the RON of the feed and product. In this procedure, at first the RON index of each species is calculated. Then, the RON of bulk is calculated by summing up the RON indexes based on the definite mixing rules.

RESULTS AND DISCUSSION

Estimated kinetic parameters using the experimental data obtained from the pilot plant of isomerization process (section 2) are presented in Table 4.

The results of modeling for different types of feed stocks (Table 2) are shown in Figs. 4 and 5. The operating conditions of all experiments are reported in Table 4. Fig. 4 shows a comparison between the model outputs and experimental molar composition of product for the first case study. This figure indicates good accuracy between the model predictions and actual values. For this case, the absolute error, sum of the absolute difference between experimental and calculated value of species mole fractions, is about 4.27%. However, the highest value of error belongs to normal pentane and isopentanes.

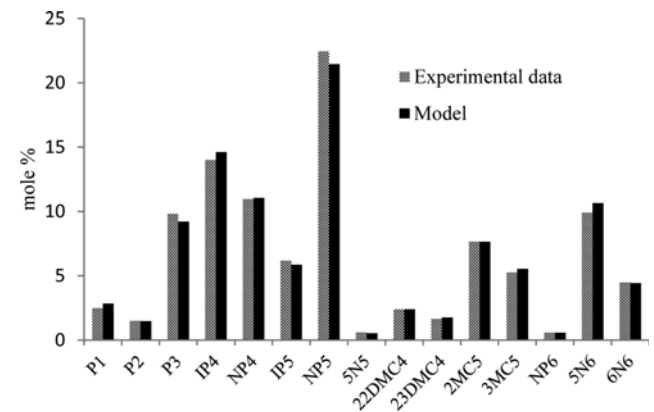
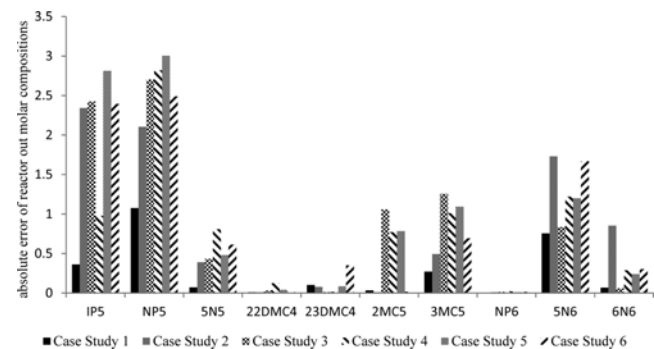
**Fig. 4. Comparison between the modeling and experimental results for the first case.****Fig. 5. Comparison between the modeling and experimental results for the first to sixth cases.**

Fig. 5 represents the capability of the model to predict the molar composition of isomerization product for other case studies (see Table 2). It is observed that the absolute error of prediction for molar compositions of species with five carbon atoms (IP5 and NP5) and methyl cyclo pentane (5NC6) was less than 3% and 1.5%, respectively. For the other components, this value is less than 1%. For example, the absolute error for normal hexane, 2, 2-dimethylbutane and 2, 3-dimethylbutane is almost zero, and for 2-methylpentane and 3-methylpentane is less than 1%.

After the model is validated, it is used for studying the effect of corresponding reactions occurring through the catalytic bed. As mentioned above, increasing the RON of feed, i.e., light naphtha is the main goal of the isomerization process, therefore, this variable is considered as an index for analyzing the performance of the reactor. Fig. 6 illustrates the effect of reactor temperature, the most important operating variable for light naphtha isomerization, on the RON of the product. This figure is obtained using the feed stock No. 2, introduced in Table 2. The presented curves are divided into three different regions. In the first, the RON of the product rises with increasing the temperature. However, in the second region, it declines with increasing the temperature. But, the trend of RON versus temperature in the third region is the same as the first one.

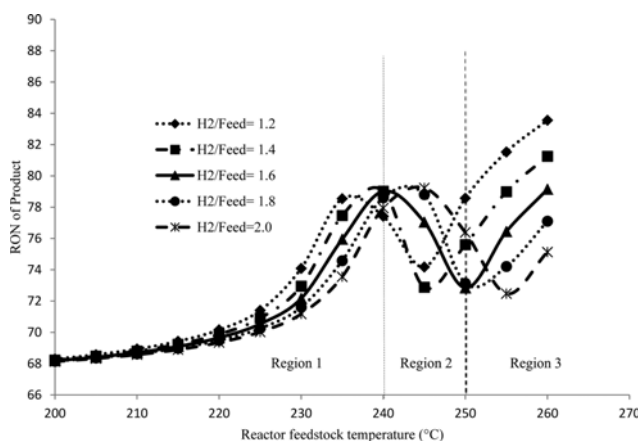


Fig. 6. The effects of reactor feedstock temperature on the composition of outlet reactor, @ LHSV=1 hr⁻¹, Feedstock no: 2 (Table 2).

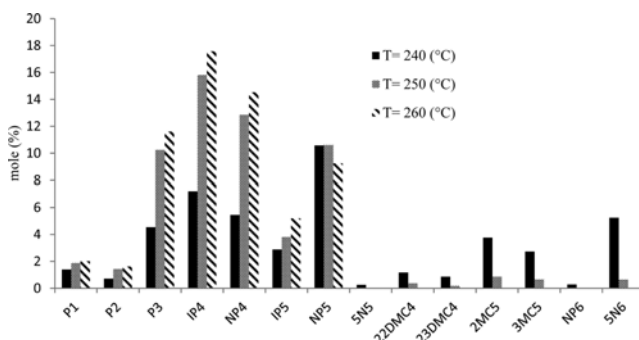


Fig. 7. The effects of reactor temperature on the composition of outlet reactor, @ Hydrogen to Feedstock molar ratio = 1.6 and LHSV=1 hr⁻¹, Feedstock no: 2 (Table 2).

It is supposed that accelerating the isomerization reactions in the first region boosts the RON to a maximum level. Decreasing the RON in the second region can be related to the accelerated hydrocracking of hydrocarbons containing six carbon atoms such as 2,2 DMC4, 2, 3 DMC4, 2MC5, 3MC5 and normal hexane. As seen from Fig. 7, by increasing the temperature from 240 °C to 250 °C, the molar percentage of the light species increases, and conversely, the heavier hydrocarbons having higher octane number decreases. Therefore, high octane number species are converted to lighter ones such as methane, propane and butanes. These light species are separated from the product in the form of fuel gas. The reduction of octane number continues until hydrocarbon species containing six carbons are hydrocracked. Finally, the upward trend of RON in the third region is due to the conversion of normal pentane to isopentane promoted at higher temperatures. Since hydrocracking reactions have a negative effect on the yield of the gasoline production, it is concluded that the optimum isomerization temperature is located in the first region in which RON and yield are both at the optimum values.

Fig. 6 also demonstrates the dependency of RON on hydrogen to hydrocarbon molar ratio when LHSV is kept constant. The optimum reactor inlet temperature depends on the hydrogen over feed molar ratio and LHSV. These results show that at constant feed flow rate, by decreasing hydrogen to feed molar ratio, the optimum reactor inlet temperature drops. It is supposed that increasing the residence time, in consequence with enhancing hydrocracking reactions is the main reason for this phenomenon. This figure also indicates that 0.4 unit increment in hydrogen-to-hydrocarbon molar ratio increases the optimum temperature about 5 °C. Fig. 8 demonstrates the effect of temperature on the yield of liquid and gas. As it declares, increasing the temperature increases the yield of gaseous products; however, it decreases the liquid yields. It confirms the impact of hydrocracking reactions. Fig. 9 illustrates the effects of LHSV on the RON of product. As seen from this figure, similarly to hydrogen to hydrocarbon molar ratio, LHSV affects the RON of the product. Indeed, the residence time increases by reducing the LHSV, and consequently the optimum reactor temperature decreases because of accelerating the hydrocracking reactions. Based on the demonstrated figures, a method can be recommended for increasing

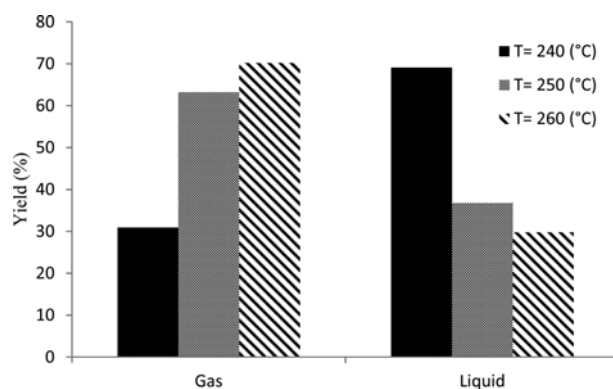


Fig. 8. The Gas and liquid product yields at different temperature @ Hydrogen to Feedstock molar ratio=1.6 and LHSV=1 hr⁻¹, Feedstock no: 2 (Table 2).

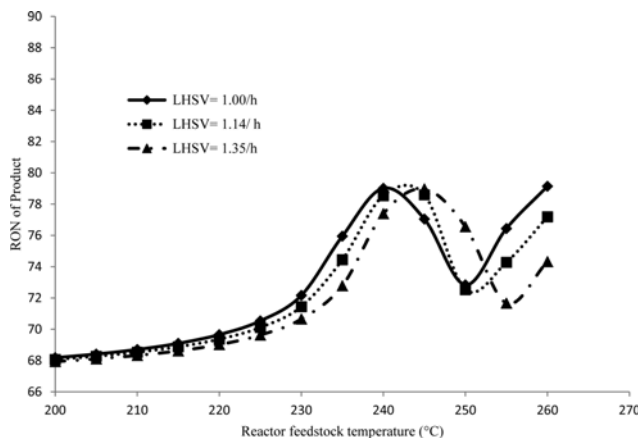


Fig. 9. The effects of inlet reactor temperature and LHSV @ hydrogen to feed molar ratio=1.6 hr⁻¹, Feedstock no: 2 (Table 2).

the capacity of light naphtha isomerization reactor. Accordingly, 5 °C increment in the reactor operating temperature increases the capacity of gasoline production while the RON of product remains at the desired value. This procedure is highly appreciated when there is limitation in increasing hydrogen to hydrocarbon molar ratio due to the process limitations such as the loading capacity of hydrogen compressor. If there is no limitation in increasing the hydrogen-to-hydrocarbon molar ratio, the reactor temperature can be elevated about 28%.

Based on this rule, if 5 °C increase in the reactor operating temperature is applied for 15% of reactor, capacity improvement the RON of product will remain constant. This is applicable while any changes of hydrogen-to-oil ratio are prohibited and there is no limitation for revamping of hydrogen compressor. However, there is no need to raise the temperature if the changing of hydrogen-to-oil ratio to more than 28% is allowed. But, an increase of hydrogen-to-oil ratio is required for less than 28% improvement in hydrogen-to-oil ratio.

CONCLUSION

Pilot scale experiments were carried out in a fixed-bed isomerization reactor using Pt/Zeolite catalyst over a wide range of operating conditions and different types of feedstock obtained from an industrial scale plant. A reaction network, including isomerization, saturation, ring opening and hydrocracking, was proposed. A rigorous kinetic model was developed for the fixed-bed reactor under study and the required adjustable parameters--activation energies and frequency factors--were estimated using the experimental data obtained from the pilot plant. The comparison between the model output and experimental data showed that the model was capable of predicting the molar composition of five and six carbon atoms species with the absolute errors of 1% and 3%, respectively.

Then, using this validated model, the impact of the hydrocracking reactions on the light naphtha isomerization was explored. Results showed when other process variables, hydrogen to feed molar ratio and LHSV, were kept constant, increasing the reactor temperature increased the RON of the product. After reaching a maximum level, RON decreased by increasing the temperature. It was supposed that the acceleration of hydrocracking reactions was the main reason for this behavior. Thereafter, by increasing the reactor temperature, RON reached a minimum level, and then increased due to the isomerization of components with five carbon atoms. According to these observations, the optimum operating temperature for producing gasoline with the maximum RON was just before performing of the hydrocracking reactions, strongly dependent on LHSV and the hydrogen-to-feed molar ratio. After increasing 28% of hydrogen-to-feed molar ratio and 14% of LHSV, the optimum temperature was raised 5 °C to compensate for the reduction of residence time in the isomerization reactor. The results may be applied to derive some rules of thumb to determine the optimum operating condition for RON maximization. As a consequence, sensitivity analysis of the operating conditions leads to determining a rule for revamping of the reactor. Thus, 5 °C increases in reactor operating temperature could compensate for the negative effect of 15% increases of reactor capacity on the RON of product while the hydrogen-to-oil ratio remains constant. However, by increasing 28% of hydrogen-to-oil molar ratio, increasing the reaction temperature for producing on-specification product with the desired RON is not necessary.

NOMENCLATURE

P1	: METHANE
P2	: ETHANE
P3	: PROPANE
IP4	: ISOBUTANE
NP4	: N-BUTANE
IP5	: 2-METHYL-BUTANE
NP5	: N-PENTANE
5N5	: CYCLOPENTANE
22DMC4	: 2,2-DIMETHYL-BUTANE
23DMC4	: 2,3-DIMETHYL-BUTANE
2MC5	: 2-METHYL-PENTANE
3MC5	: 3-METHYL-PENTANE
NP6	: N-HEXANE
5N6	: METHYLCYCLOPENTANE
A6	: BENZENE
6N6	: CYCLOHEXANE
2MC6	: 2-METHYLHEXANE
3MC6	: 3-METHYLHEXANE
w _i	: weighting factor
x _i	: components mole fraction
m	: reaction order
k _{f,n}	: frequency factor of forward reaction ([kgmol/m ³] ^{1-m} *S ⁻¹)
k _{r,n}	: frequency factor of reverse reaction ([kgmol/m ³] ^{1-m} *S ⁻¹)
E _{f,n}	: activation energy of forward reaction [kJ/kgmole]
E _{r,n}	: activation energy of reverse reaction [kJ/kgmole]

REFERENCES

1. A. D. Estrada-Villagrana and C. Paz-Zavala, *Fuel*, **86**, 1325 (2007).
2. S. Sadighi, S. Zahedi, R. Hayati and M. Bayat, *Energy Technol.*, **1**(12), 743 (2013).

3. P. Leprine, Conversion Processes, Editions Technip. (2001).
4. J. R. H. Ross, *Heterogeneous Catalysis*, Elsevier (2012).
5. R. G. Tailleux and J. B. Platin, *J. Catal.*, **255**(1), 79 (2008).
6. S. Sadighi, A. Ahmad and M. Shirvani, *Chem. Eng. Technol.*, **35**(5), 919 (2012).
7. K. Watanabe, N. Chiyoda and T. Kawakami, *18th Saudi Arabia-Japan Joint Symposium Dharan*, Saudi Arabia, November 16-17 (2008).
8. R. Issadi, F. Garin and C. E. Chitour, *Catal. Today*, **113**, 174 (2006).
9. R. G. Tailleux and C. Albornoz, *Catal. Today*, **150**, 308 (2010).
10. K. Wantabe, T. Kawakami, K. Baba, N. Oshio and T. Kimira, *Appl. Catal. A: Gen.*, **276**, 145 (2004).
11. S. Zahedi Abghari, J. Towfighi Darian, R. Karimzadeh and M. R. Omidkhan, *Korean J. Chem. Eng.*, **25**(4), 681 (2008).
12. S. Sadighi, A. Ahmad and M. Rashidzadeh, *Korean J. Chem. Eng.*, **27**(4), 1099 (2010).
13. S. Zahedi Abghari, S. Shokri, B. Baloochi, M. Ahmadi Marvast, S. Ghanizadeh and B. Afshin, *Korean J. Chem. Eng.*, **28**(1), 93 (2011).
14. J. Sadeghzadeh Ahari, S. J. Ahmadpanah, A. Khaleghinasab and M. Kakavand, *Petroleum Coal*, **47**(3), 26 (2005).
15. E. A. Medina and J. I. P. Paredes, *Math. Comp. Model.*, **49**, 207 (2009).
16. K. Surla, H. Vleeming, D. Guillaume and P. Galtier, *Chem. Eng. Sci.*, **59**, 4773 (2004).
17. A. Bernas and D. Y. Murzin, *Chem. Eng. J.*, **115**, 23 (2005).
18. F. Sandelin, T. Salmi and D. Yu. Murzin, *Ind. Eng. Chem. Res.*, **45**, 558 (2006).
19. H. S. A. Douwes, *J. Mol. Catal. A: Chem.*, **272**, 220 (2007).
20. M. Khurshid and S. Al-Khattaf, *Appl. Catal. A: Gen.*, **368**, 56 (2009).
21. N. V. Chekantsev, M. S. Gyngazova and E. D. Ivanchina, *Chem. Eng. J.*, **238**, 120 (2014).
22. J. Ancheyta, *Modeling and simulation of catalytic reactors for petroleum refining*, Wiley (2011).
23. D. S. G. Jones and P. R. Pujado, *Handbook of petroleum processing*, Springer (2006).
24. S. Parkash, *Refining processes handbook*, Elsevier (2003).
25. M. A. Fahim, T. A. Alsahhaf and A. Elkilani, *Fundamental sof petroleum refining*, Elsevier (2010).
26. M. R. Riazi, *Characterization and properties of petroleum fractions*, ASTM International Publishing (2005).